Adhesive Placement in Weld-Bonding Multiple Stacks of Steel Sheets

An understanding of and guidelines for weld-bonding multiple stacks of steel sheets were developed

BY J. SHEN, Y. S. ZHANG, X. M. LAI, AND P. C. WANG

ABSTRACT

Weld-bonding technology has been widely used in vehicle manufacturing to improve structural crashworthiness, fatigue performance, and corrosion resistance. This study focused on the weld quality in weld-bonding multiple stacks of steel sheets composed of 0.8-mm-thick SAE1004, 1.4-mm-thick DP600, and 1.8-mm-thick DP780 with various adhesive placements. To investigate the effect of the adhesive placement on the weld-bonding process, the static contact and dynamic resistances between the steel sheets with adhesive were measured. Then, the weld formation, weld size, and hardness of weld-bonded joints with various adhesive placements were studied by metallographic tests. Results showed that the static contact and dynamic resistances between the steel sheets increased significantly due to the presence of the adhesive. The weld initiation time and weld size for weld-bonded joints were about 40 ms earlier and 10% larger than that without adhesive under the same welding parameters. Weld qualities of weld-bonded joints with two adhesive layers at both faying interfaces between multiple stacks of steel sheets produced the best. This study provides the guidelines to the application of adhesive in weld-bonding multiple stacks of steel sheets for vehicle manufacturing.

Introduction

The weld-bonding process, which is a combination of resistance spot welding (RSW) and adhesive bonding, produces more desirable joint performance when compared to either spot welding or adhesive bonding (Refs. 1–3). It not only improves the crashworthiness, stiffness, fatigue behavior, and corrosion resistance (Refs. 4, 5), but also enables a reduction in the number of welds used in vehicle structures. Therefore, this joining technology has been widely applied in vehicle bodies such as front longitudinal rails; A, B, and C pillars; and the bulkhead to inner wing. However, due to the complexity of the multiple stacks of steel sheets often encountered in vehicle assembly, the effect of the adhesive placement is not well documented (e.g., one adhesive layer between two steel sheets, two adhesive layers in three sheets). Therefore, the benefits of weld-bonding multiple stacks of steel sheets for vehicle assembly applications have not been fully maximized.

Many studies have been reported on the weld-bonding of two steel sheets (Refs. 6, 7). Studies have shown that the adhesive increased the weld size and strength in weld-bonded joints compared to resistance spot welds under the same welding parameters (Ref. 8). Although extensive studies have been done on weld-bonding two steel sheets, little work has been reported on weld-bonding multiple stacks of steel sheets. Because there are many joint configurations and designs on a body-in-white structure, it is conceivable that weld-bonding multiple stacks of workpieces is inevitable. Therefore, it is essential that an understanding of weld-bonding of multiple steel sheets be obtained. The present study was undertaken to experimentally and analytically evaluate the effect of the adhesive placement on the weld quality in weld-bonding multiple stacks of workpieces.

Because the adhesive is placed between the steel sheets, the initial contact state and contact resistance between them would be changed and conceivably, the quality of the weld nugget might be affected. Previous studies have shown that the contact state and contact resistance between the steel sheets significantly affect the weld-bonding process (Refs. 9–12). During the weld-bonding process, the contact resistance distribution influences the current density pattern, which affects the temperature field through Joule heating. The temperature field then influences the mechanical pressure distribution through thermal expansion of the workpieces. Therefore, the formation of the weld nugget is indeed strongly dependent on the phenomena at the faying interfaces. Meanwhile, the placement of the adhesive between the workpieces changes the contact state between them because of the viscosity and heat insulation, and consequently affects the weld formation and weld quality. To investigate the weld formation process, the dynamic resistance, which is a comprehensive resistance of the welding joint containing the bulk and contact resistance of the steel sheets, is used as one of the most widely accepted procedures (Refs. 13–16). We

KEYWORDS

Weld-Bonding Process
Multiple Stacks
Nugget Formation
Adhesive Placement

J. SHEN, Y. S. ZHANG (zhangyansong@sjtu.edu.cn), *and X. M. LAI are with the Shanghai Key Lab for Digital Auto-Body Engineering, State Key Lab of Mechanical System and Vibration, Shanghai Jiao Tong University, Shanghai, China. P. C. WANG is with the Manufacturing Systems Research Lab, General Motors Research & Development Center, Warren, Mich.*

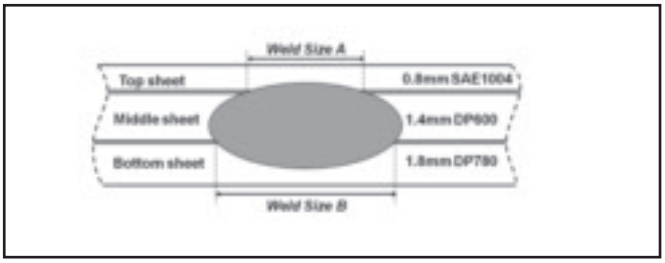

Fig. 1 — Weld nugget configuration in weld-bonding multiple stacks of steels.

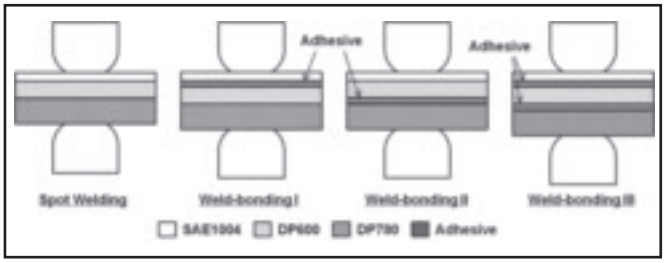

Fig. 2 — Various adhesive locations in weld-bonding three sheets.

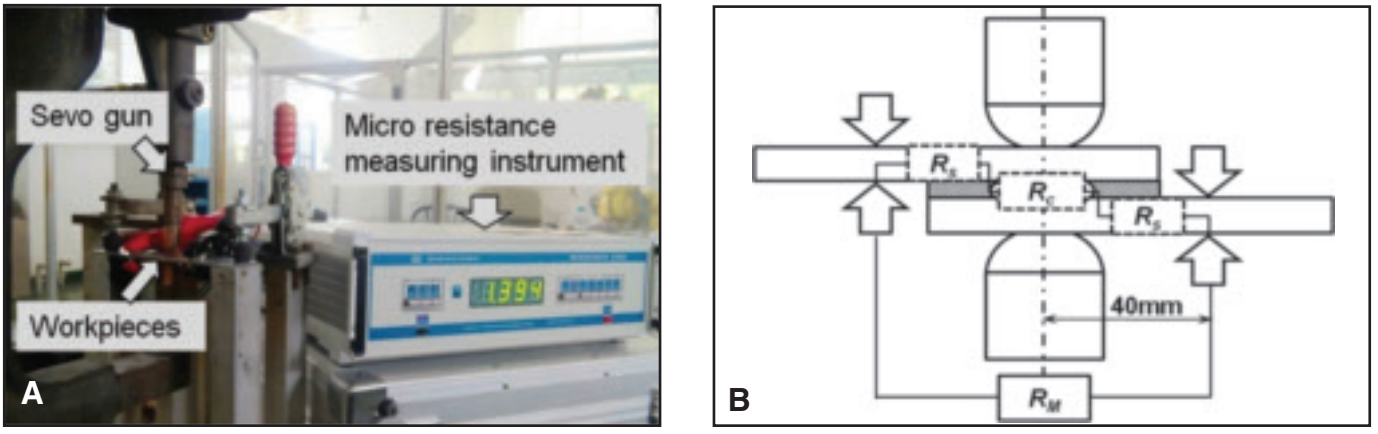

Fig. 3 — Experimental setup for measuring the static contact resistance between the steel sheets and adhesive. A — Test setup; B — resistances between the steel sheets.

Table 1 — Chemical Composition and Mechanical Properties of Various Steels

Steel	Chemical Composition (%)						Mechanical Properties		
	C	Mn	P	S	Si	Al	Yield Strength (MPa)	Tensile Strength (MPa)	Elongation (%)
SAE1004	0.037	0.21	0.01	0.02	0.018	0.04	152	278	66
DP600	0.08	1.74	0.012	0.003	0.016	0.041	316	607	29
DP780	0.15	1.80	0.004	0.016	0.010	0.048	508	834	26

Table 2 — Adhesive Properties of Terokal 5089

Solids Content	Specific Gravity	Viscosity @ 50°C (Pa·s)
>98.5%	1.05~1.20	30–50

apply the same approach to assess the effect of the adhesive placement on weld-bonding multiple stacks of steel sheets.

There are three main parts in this report. The first presents the experimental procedure including material, experimental setup, sample fabrication, and weld characterization. In the next section, the experimental results where the effect of the adhesive placement on the static and dynamic resistances during weld bonding are reported. The calculated effect of adhesive placement on the temperature distribution is then presented. Finally, the effect of the adhesive placement on the weld size and hardness of the weld-bonding joint with various adhesive placements is discussed. This work provides valuable guidelines to the application of adhesive in weld-bonding multiple stacks of steel sheets for vehicle manufacturing.

Experimental Procedure

Materials

To investigate weld-bonding multiple stacks of steel sheets, 0.8-mm-thick, hot-dipped galvanized (HDG), low-carbon steel SAE1004, 1.4-mm-thick (HDG) DP600, and 1.8-mm-thick (HDG) DP780 steels were used in this study. All have the coating thickness of 60 g/m^2. The chemical composition and mechanical properties of these steels are measured and listed in Table 1.

An epoxy resin-based adhesive (Terokal 5089) manufactured by Henkel was used in this study. It is a one-component, hot-cured adhesive with low viscosity before curing and high performance after curing. The material properties of Terokal 5089 from the Henkel data sheet are listed in Table 2.

Experimental Setup and Sample Fabrication

The weld-bonding process is realized by use of a servo gun welding system having a medium-frequency direct current (MFDC) welding machine. The servo gun can precisely control the welding force of

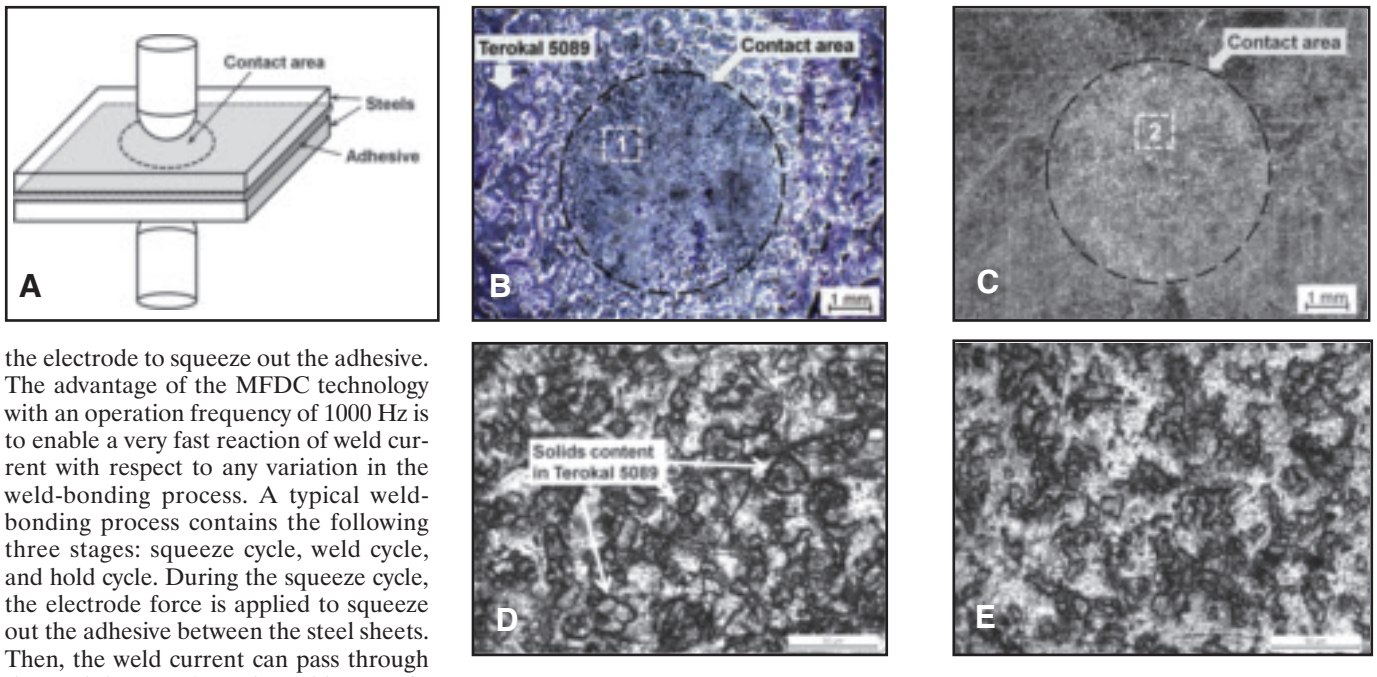

Fig. 4 — Effect of adhesive on the contact state in weld-bonding 0.8-mm-thick galvanized SAE1004 steel. A — Contact area between workpieces after squeezing; B — residual adhesive between the workpieces; C — contact area without adhesive; D — enlarged view of area 1 in B; and E — enlarged view of area 2 in C.

the electrode to squeeze out the adhesive. The advantage of the MFDC technology with an operation frequency of 1000 Hz is to enable a very fast reaction of weld current with respect to any variation in the weld-bonding process. A typical weld-bonding process contains the following three stages: squeeze cycle, weld cycle, and hold cycle. During the squeeze cycle, the electrode force is applied to squeeze out the adhesive between the steel sheets. Then, the weld current can pass through the steel sheets to form the weld nugget in the weld cycle. A weld-bonding joint could finally be completed after the cooling in the hold cycle.

In this study, the multiple stacks of three sheets is composed of 0.8-mm-thick SAE1004 as the top sheet, 1.4-mm-thick DP600 as the middle sheet, and 1.8-mm-thick DP780 as the bottom sheet — Fig. 1. The adhesive layer of Terokal 5089 first is laid on the steel sheets, and then the welding current is applied through the adhesive and steels to get a weld-bonding joint. Class II copper alloy with chromium and zirconium electrode is used in the experiment, and the welding parameters are listed in Table 3.

For a multiple stack weld-bonding joint with 0.8-mm-thick SAE1004, 1.4-mm-thick DP600 and 1.8-mm-thick DP780 from top to bottom sheet, there would be three different types of weld bonding according to the different adhesive locations as given in the schematic of Fig. 2. The joint without adhesive is traditional resistance spot welding. Weld-bonding type I represents a joint with one adhesive layer on the interface between SAE1004 and DP600. Similarly, weld-bonding type II represents a joint with one adhesive layer between the DP600 and DP780 sheets and weld-bonding type III represents a joint with two adhesive layers between three steel sheets.

Weld Characterization

Because of the stack-up joint's complexity, the traditional weld dimension (diameter in the center of the weld nugget) cannot clearly characterize the quality and shape of the weld nugget in weld-bonding of three sheets. Hence, a new weld configuration with a typical dimensional parameter for a joint with multiple stacks is presented in Fig. 1. There are two critical dimensions of the weld nugget — weld sizes A and B. Weld size A can represent the joint quality between the top and middle sheets. Weld size B represents the connection between the middle and bottom sheets. These two weld sizes can be measured from the micrographs of the joint cross section, which is prepared for measurement using Nital 4% etch applied after mechanical grinding and polishing. The thicknesses of the top and middle sheets are 0.8 and 1.4 mm, respectively; the minimum dimension for weld size A is set at 4.0 mm (Ref. 17). Similarly, the minimum weld size B is 5.0 mm. After the metallographic test, the Vickers hardness tests were conducted using a 200-g load and hold time of 10 s. Five replicates were prepared for the metallographic and hardness tests.

Results and Discussion

Static Contact Resistance during Squeeze Cycle

The first stage of the weld-bonding process is the squeeze cycle. During the squeeze cycle, an electrode force is applied to clamp the sheets together, which has the effect of squeezing out the adhesive between the steel sheets and creating intimate contact making it easier for the welding current to pass through. In order to investigate the contact state (including the adhesive distribution and static contact resistance) between the steel sheets with the adhesive layer, a measurement system in Fig. 3A was set up with a micro resistance measuring instrument and the servo gun. This system is capable of measuring the static contact resistance between the steel sheets with different contact forces in the precision of 0.1 μΩ. The measurement principle, presented in Fig. 3B, is based upon R_M, which is the total resistance between two fixtures installed at 40 mm from the centerline of the electrode and can be directly measured by the system. R_S is the bulk resistivity of the steel sheets from the contact region to the fixture, which is a constant value at ambient temperatures. R_C is the static contact resistance between the steel sheets. According to the setup in Fig. 3B, the static contact resistance R_C can be calculated by Equation 1.

$$R_C = R_M - 2R_S \quad (1)$$

During the squeeze cycle, an electrode force is applied to clamp the sheets together, which has the effect of squeezing out the adhesive between the steel sheets and creating intimate contact. Figure 4A shows the contact area between the steel sheets after squeezing. Figure 4B and D are the state of the adhesive on the interface between two 0.8-mm-thick SAE1004 steel sheets after the squeeze cycle with an electrode force of 5.5 kN. As shown in Fig. 4B, there is a distinct difference in adhesive distribution between the area of contact and outside of the contact area.

Area 1 is the contact surface where

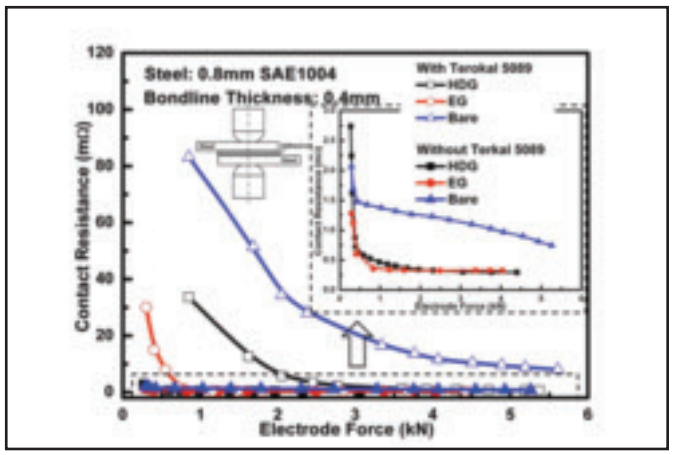

Fig. 5 — Effect of the coating on the static contact resistance in resistance welding and weld-bonding 0.8-mm-thick SAE1004 steel.

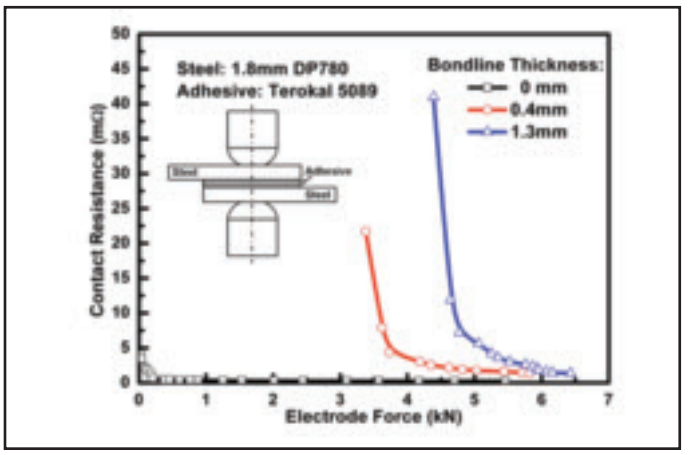

Fig. 6 — Effect of adhesive bondline thickness on the static contact resistances in weld-bonding 1.8-mm-thick DP780 steel.

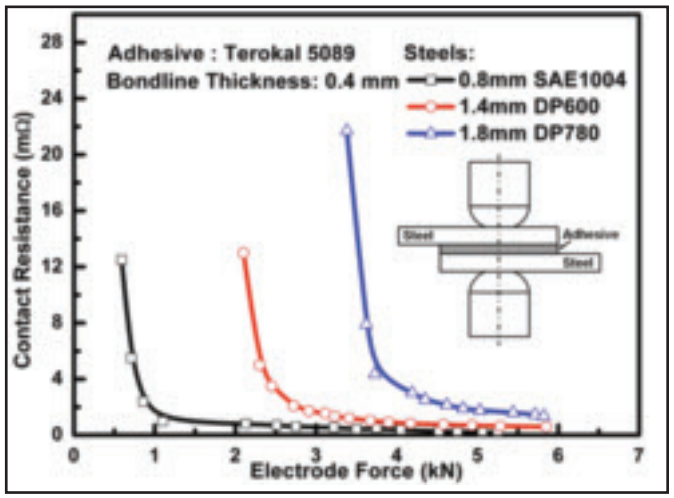

Fig. 7 — The static contact resistances of 0.8-mm-thick SAE1004, 1.4-mm-thick DP600, and 1.8-mm-thick DP780 in weld bonding.

there is some residual adhesive sticking to the steel surface after the squeeze cycle. A closer examination of Fig. 4B is given in Fig. 4D and shows evidence of granular solids in the adhesive layer in area 1 even though an electrode force of 5.5 kN is applied.

Experimental observations showed that the amount of residual adhesive left on the contact surfaces depends on the composition and viscosity of the adhesive, electrode force, and ambient temperature. On the contrary, Fig. 4C and E exhibit a clear contact surface of a zinc-coated SAE1004 steel (HDG60) without adhesive. Comparing the steel surfaces with and without adhesive shown in Fig. 4, it is clearly demonstrated that the adhesive interferes with the contact state between the steel sheets, which could influence the static contact resistance in weld bonding the workpieces.

Figure 5 shows the effects of the coating and electrode force on the static contact resistance of two 0.8-mm-thick SAE1004 steel sheets with adhesive Terokal 5089. To assess the effect of the coating, steels with various coatings were used in the experiments. It could be seen that without the presence of the adhesive, the hot-dipped galvanized (HDG) and electrogalvanized (EG) steel sheets have smaller static contact resistance than does bare steel sheet. This is attributed to the fact that the zinc coating has a relatively high electrical conductivity, and consequently contributes to the reduction of the total contact resistance between the steel sheets. However, when the adhesive is placed between the steel sheets, the static contact resistance significantly increases as exhibited by the bare SAE1004 with adhesive having the largest contact resistance. Within the selected range of surface coating and adhesive, the change in static contact resistance caused by surface coating is negligible compared to the presence of the adhesive. These results suggest that the adhesive has the greatest effect on the static contact resistance between the steel sheets by sticking to the sheet surface.

To investigate the effect of the adhesive thickness on the static contact resistance between the steel sheets, experiments were performed using 1.8-mm-thick DP780 steel, and the results are shown in Fig. 6. The results show that the static contact resistance without adhesive (bondline thickness = 0 mm) is small up to an electrode force of approximately 0.5 kN. However, the presence of the adhesive between the steel sheets significantly increases the static contact resistance. The static contact resistance increases with the adhesive bondline thickness; however, this effect diminishes as the electrode force increases. As the electrode force reached about 6.0 kN, the static contact resistance virtually becomes a constant. These results suggest that a large electrode force is required for the thick adhesive to conquer the viscosity of the adhesive sandwiched between the steel sheets. Once the excessive adhesive was squeezed out, the static contact resistance between steel sheets reached a stable state.

A minimum electrode force is needed to squeeze out the adhesive and then maintain the workpieces in intimate contact. Figure 7 shows the static contact resistances of 0.8-mm-thick SAE1004, 1.4-mm-thick DP600, and 1.8-mm-thick DP780 used in this study. The adhesive is Terokal 5089 with a thickness of 0.4 mm. As can be observed for a given electrode force, the 1.8-mm-thick DP780 steel has the largest static contact resistance with adhesive, which is attributed to the large bulk resistivity of DP780 compared to SAE1004 and DP600 steels (Ref. 18). For

Table 3 — Welding Parameters for Stack-Up Joint

Electrode Diameter (mm)	Electrode Force (kN)	Welding Current (kA)	Time (ms)		
			Squeezing	Welding	Hold
5.0	5.5	9.0	200	420	100

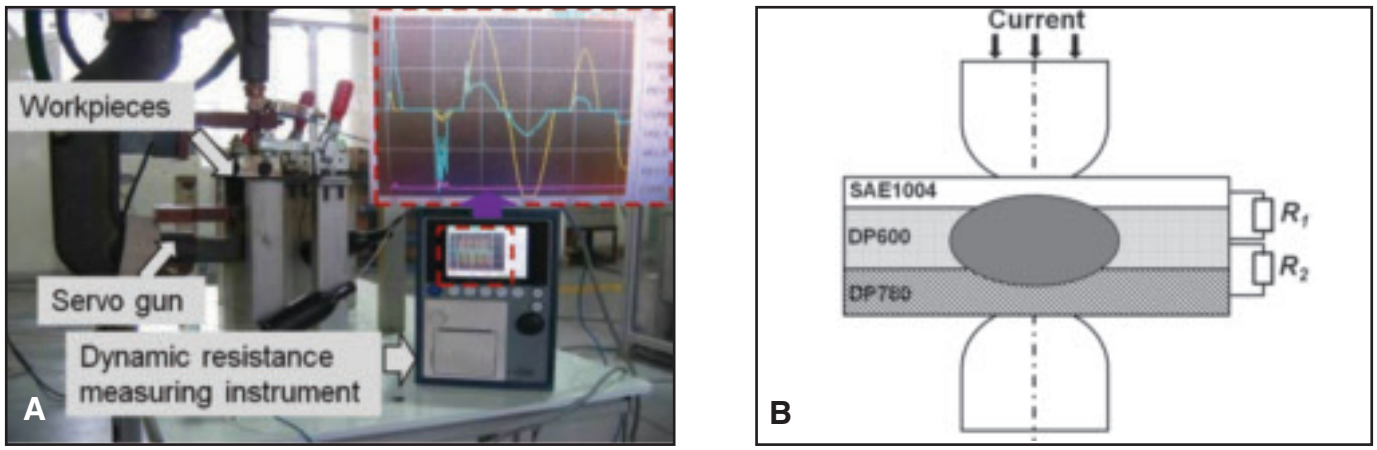

Fig. 8 — Measurement of dynamic resistance between the workpieces. A — Test setup; B — dynamic resistance R_1 and R_2 between the workpieces.

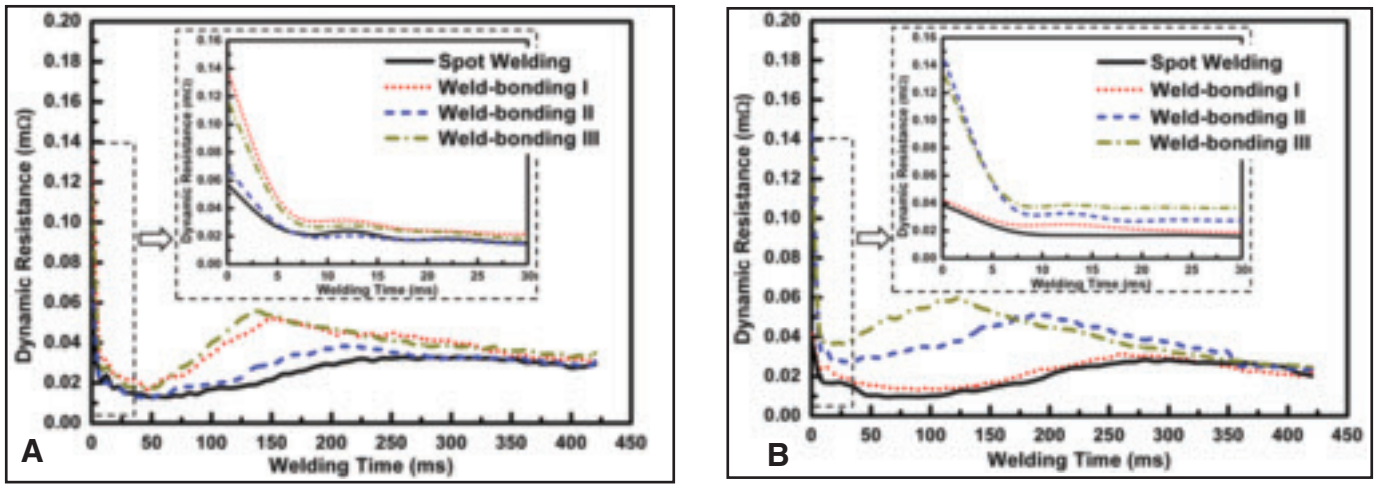

Fig. 9 — Dynamic resistances between workpieces during weld-bonding. A — R_1 between the top and middle sheets; B — R_2 between the middle and bottom sheets.

the three steel sheets in this study, it is effective to decrease the static contact resistance by increasing the electrode force. The minimum electrode force to keep the static contact resistance stable is different because of the various thicknesses and moduli of the steel sheets. An electrode force of 1.1 kN for SAE1004 (0.8-mm-thick), 3.1 kN for DP600 (1.4-mm-thick), and 4.6 kN for DP780 (1.8-mm-thick) are required for weld-bonding.

Dynamic Resistance during Weld Cycle

After the squeeze cycle, the weld current is applied to the workpieces through the electrodes to start the weld cycle. During this stage, the properties of the steel sheets and adhesive change with the temperature rise resulting from the generation of the Joule heat. When the temperature goes up to about 1500°C, a molten weld nugget forms. The dynamic resistance has been used to study the weld formation during the welding process. A typical dynamic resistance curve during welding contains three stages (Ref. 17). In the first stage during the beginning of welding, the dynamic resistance drops due to the decrease of the static contact resistance between the steel sheets because of the temperature rise. After that, the dynamic resistance goes up with the rise of the bulk resistivity of the steels by temperature in the second stage. Finally, the dynamic resistance becomes stable and decreases slightly in the third stage because of the formation of the weld nugget.

In our study, we measured the dynamic resistance to investigate the weld formation in weld bonding. Figure 8A is a photo of the experimental setup used to measure the dynamic resistance. The weld current and voltage data between the steel sheets were collected using the welding monitor (MM-370A) made by Miyachi. To assess the effect of the adhesive placement, the dynamic resistances on two interfaces between the steel sheets were measured. Figure 8B is a schematic of the measurement method where R_1 is the dynamic resistance between the top and middle sheets, and R_2 is the dynamic resistance between the middle and bottom sheets. Five replicates were performed for each type of weld bonding, and the average dynamic resistances were reported.

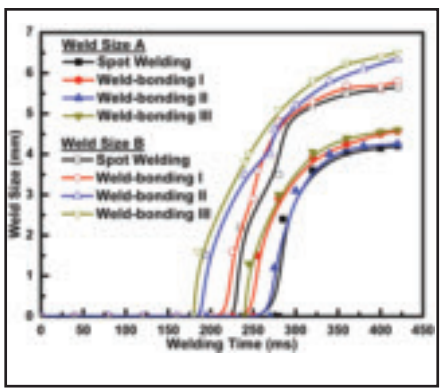

Fig. 10 — Weld formation for different types of weld bonding.

During the weld cycle, a welding current of 9.0 kA is applied to start the joining process. The measurements of dynamic resistance (R_1) between the top and middle sheets during welding are provided

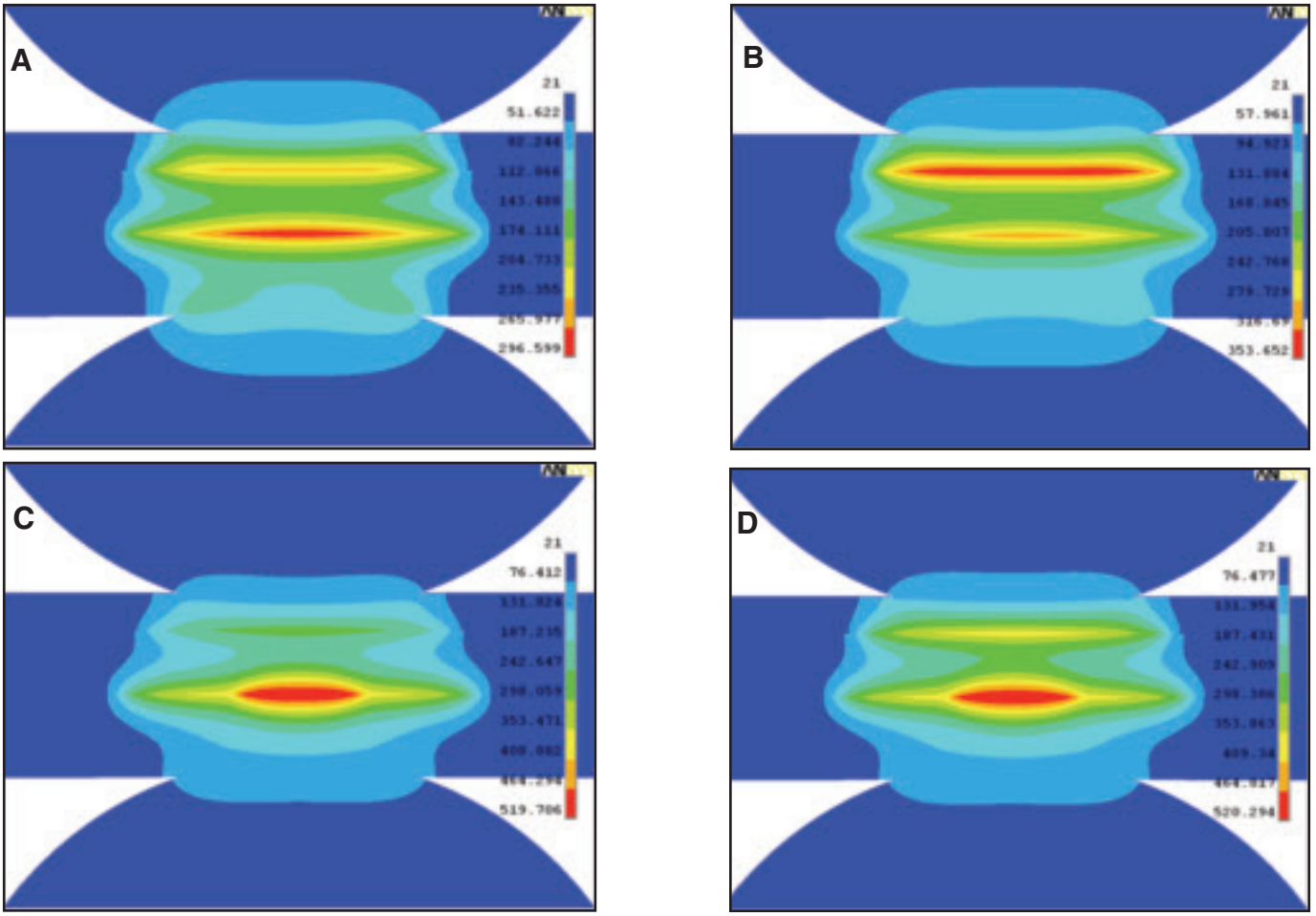

Fig. 11 — Initial temperature distributions with different adhesive locations. A — Spot welding; B — weld-bonding I; C — weld-bonding II; and D — weld-bonding III (welding time = 20 ms).

in Fig. 9A. Because there is no adhesive layer at the interface between the top and middle sheets in resistance spot welding and weld-bonding type II, the dynamic resistance results for this specific interface during the whole weld-bonding process are similar because of comparable contact conditions. However, when the adhesive is placed in this interface as defined by weld-bonding types I and III, the dynamic resistance results during the first and second stage are larger than those without adhesive, especially during the welding time from 50 to 250 ms. This is attributed to the fact that the residual adhesive left between the top and middle sheets after squeezing increased the static contact resistance. Under the same welding current during the weld cycle, additional Joule heat would be generated, thereby causing the temperature of the steel sheets to rise faster than if no adhesive is present. The rapid rise of temperature would, in turn, increase the bulk resistivity of the steel sheets. As a result, the dynamic resistances between the top and middle sheets of weld-bonding types I and III would be larger than those of spot welding and weld-bonding type II under the same welding conditions.

Similar results in Fig. 9B were found for the dynamic resistances between the middle and bottom sheets (R_2) during welding. The spot welding and weld-bonding type I had similar dynamic resistances because there is no adhesive at this interface between the steel sheets. The dynamic resistances R_2 of weld-bonding types II and III are larger than those of spot welding and weld-bonding type I because of the application of the adhesive on the interface between the middle and bottom sheets. It could also be seen in Fig. 9 that weld-bonding type III has the largest dynamic resistance on both interfaces during the welding time from 50 to 150 ms. This is attributed to the fact that the heat generation at the two interface influences combine to cause the greater rise in temperature compared to the others during the weld cycle.

Weld Formation during Welding

The variations in dynamic resistance could indicate a change in weld formation during the weld-bonding process. Figure 10 is a plot of the weld size at each of the two interface locations in the three-sheet stack-up (represented by weld sizes A and B shown in Fig. 1) for different types of weld bonding. As can be seen in Fig. 10, weld size A of weld-bonding types I and III initiates at 230 ms, which is slightly earlier than that for spot welding and weld-bonding type II (270 ms). Similar results were also found for the formation of weld size B at the interface between the middle and bottom sheets with adhesive (Terokal 5089), which initiated approximately 40 ms earlier than the case without adhesive. As a result, the final weld sizes A and B are affected by the increase of static contact resistance between the sheets caused by the application of the adhesive. It could also be seen that for all types of weld-bonding, the weld nugget on the interface between the middle (DP600) and bottom sheets (DP780) initiates earlier and is bigger than that on the other interface. This is because the greater bulk resistivity of thick DP600 and DP780 steels leads to a rapid temperature rise by the Joule heat as compared to SAE1004.

To understand the early initiation of the weld nugget for the case where the adhesive is present between the workpieces

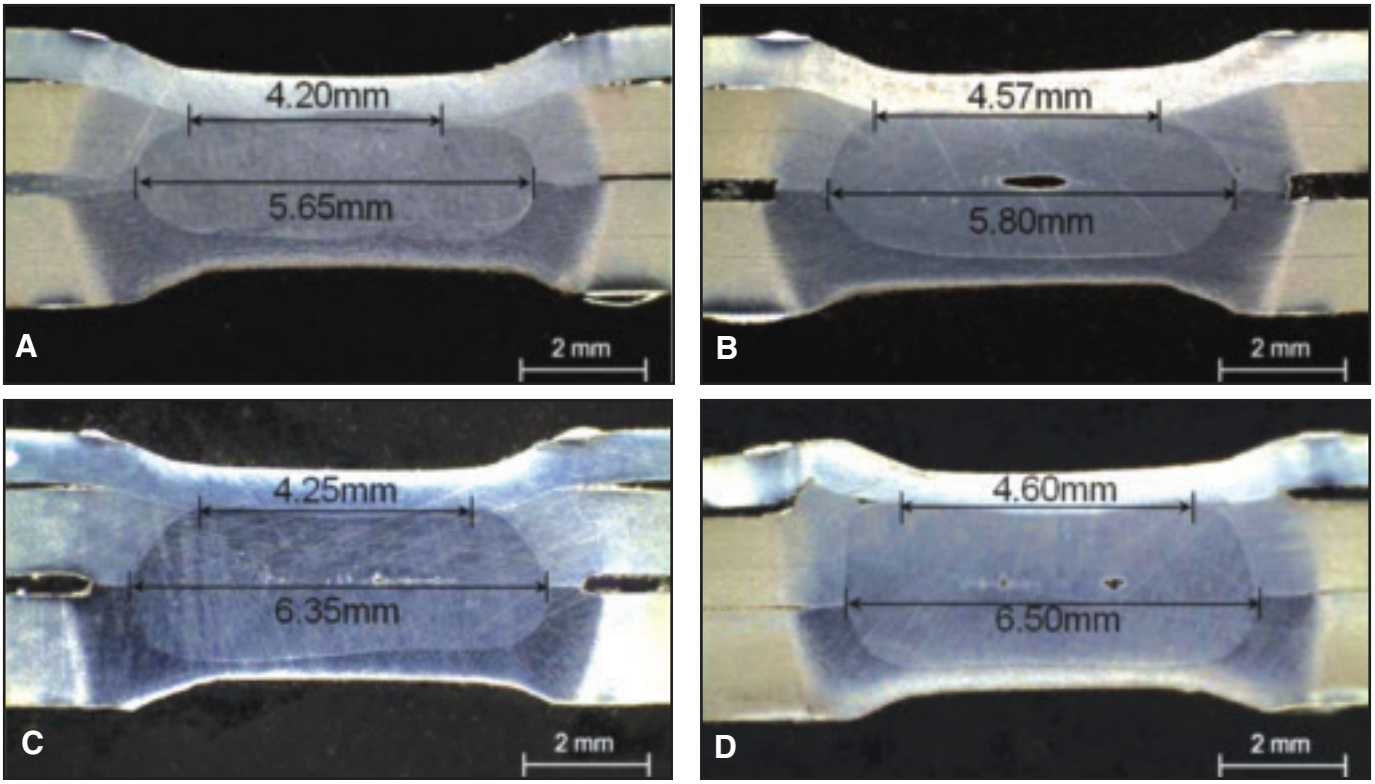

Fig. 12 — Effect of adhesive placement on the weld size. A — No adhesive (spot welding); B — weld-bonding type I; C — weld-bonding type II; and D — weld-bonding type III.

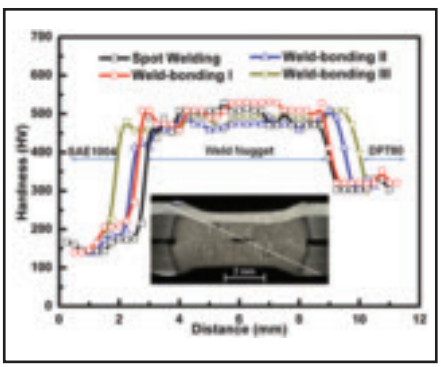

Fig. 13 — Effect of adhesive location on the hardness in weld-bonding multiple workpieces.

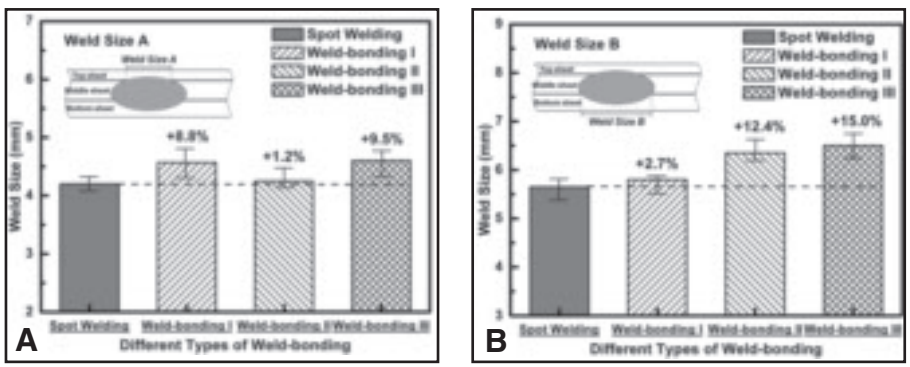

Fig. 14 — Effect of adhesive location on the weld size. A — Weld size A; B — weld size B.

during welding, a finite element model has been employed to model the weld-bonding process (Ref. 19). The presence of the adhesive was modeled as additional electrical contact resistance between the steel sheets (Ref. 20). Figure 11 shows the calculated initial temperature field for different types of weld-bonding at a welding time of 20 ms during the weld cycle. As shown in Fig. 11A, an elevated temperature has built up at the two faying interfaces between the multiple stacks of steel sheets during spot welding. More Joule heat is generated around the interface between the middle-to-bottom sheet interface due to the large static contact resistance and bulk resistivity of DP600 and DP780, compared to SAE1004. However, when the adhesive is placed on the top-to-bottom sheet interface in weld-bonding type I (Fig. 11B), the maximum temperature location has switched from the middle-to-bottom sheet interface to the top-to-middle sheet interface. Figure 11C shows that the heat generation for the weld-bonding type II where the heat has built up at the middle-to-bottom sheet interface with less heat at the top-to-middle sheet interface. Similar results were observed in Fig. 11D for the weld-bonding type III. One can conclude from these results that the presence of the adhesive increases the static contact resistance between the steel sheets, and consequently generates more Joule heat at the interfaces with adhesive. The Joule heat generation and localized temperature distribution resulting from the application of the adhesive leads to the rapid rise of the temperature of the steel sheets to the melting point (approximately 1500°C). As a result, the weld nugget on the interface with adhesive initiated early.

Weld Size and Hardness

The placement of the adhesive changes the weld initiation and formation so that the weld quality might differ for each weld-bonding type. Weld size is an important index to evaluate the quality of weld-bonding multiple stacks of steel sheets. Figure 12 is a series of photos of the metallographic cross sections taken from different types of weld-bonded joints produced with the welding parameters listed in Table 3. It can be observed that the weld sizes A and B of weld-bonded type III joints are the largest. Comparing the results of spot welded and weld-bonded type

I joints, the weld size A increases from 4.20 to 4.57 mm because of the presence of the adhesive, while the weld size B changes little, which is to be expected because there is no adhesive in either case. The opposite phenomenon occurred in the weld-bonded type II joint, which is consistent with the previous results that the placement of adhesive increases the static contact resistance between the steel sheets and initiated the weld nugget earlier. Therefore, resistance welding of the workpieces with adhesive generates more Joule heat.

Beside the weld sizes, the microstructure of the weld nugget was also examined to assess the weld quality of the weld-bonded joint. To investigate the effect of the adhesive on the microstructure of the weld nugget in weld bonding, the Vickers hardness along an oblique line through the top to bottom sheet was measured, and the results are presented in Fig. 13. The results show that the hardness of the SAE1004 is approximately 150 HV, refer to distance 0–2 mm. The hardness of the DP780 steel is approximately 300 HV, refer to distance 10–12 mm, which is significantly greater than that of the ferritic structure of the SAE1004 because of the DP780 microstructure containing martensite and ferrite. The center portion of the measurements is the hardness of the weld nugget, whose hardness is significantly greater than either of the base metals because it is fully martensitic. It should be noted that the hardness of the weld nugget is nearly the same in all kinds of weld bonding, which means that the weld nugget microstructure is not a function of the adhesive presence. However, the distribution of hardness in weld-bonding type III is the widest of the various types of weld bonding, which suggest that the weld-bonded type III joints have the largest weld size.

To determine the increase in weld size by the presence of the adhesive in weld bonding, five duplicates for each weld-bonding type were measured metallographically. Figure 14 is a graph of the average weld sizes for the various types of weld bonding under identical welding parameters. It can be observed that the presence of adhesive in weld-bonding types I and III results in an approximately 9% increase in weld size A as compared to spot welding. The weld-bonding types II and III exhibit an increase of 12.4 and 15.0%, respectively, as compared to spot welding for weld size B. For both weld sizes, weld bonding without adhesive at the interface between the sheets is comparable to spot welding (i.e., weld size A in weld-bonding type II and weld size B in weld-bonding type I). By comparing the weld sizes with various placements of the adhesive layer, the weld quality of weld-bonding type III is the best.

Conclusions

1. The static contact resistance between the steel sheets during the squeeze cycle in weld bonding is higher than that in resistance welding due to the presence of the adhesive.

2. To achieve the intimate contact between the steel sheets, a minimum electrode force is required in resistance welding of steels. The forces of 1.1, 3.1, and 4.6 kN are required for 0.8-mm-thick SAE1004, 1.4-mm-thick DP600, and 1.8-mm-thick DP780, respectively.

3. The temperature distribution is localized at the faying interface between the steel sheets with the placement of the adhesive during the welding cycle. The dynamic resistance between the steel sheets in the weld-bonding process increases compared to the resistance spot welding because of the rapid rise of temperature.

4. The weld initiation time and weld size for weld-bonded steels composed of 0.8-mm-thick SAE1004, 1.4-mm-thick DP600, and 1.8-mm-thick DP780 are about 40 ms earlier and 10% larger than that without adhesive under the same welding parameters.

Acknowledgments

This research was supported by the General Motors Collaborative Research Laboratory at Shanghai Jiao Tong University, the Research Fund of State Key Lab of MSV, China (Grant No. MSV-2010-04), and Project 50905111 supported by the National Natural Science Foundation of China. The authors gratefully acknowledge the financial and technical support provided by GM-Research and Development to carry out the present work.

References

1. Jones, T. B. 1995. Weld-bonding — The mechanism and properties of weldbonded joints. *Sheet Metal Industries* 72(9): 30, 31.

2. Chang, B. H., Shi, Y. W., and Dong, S. J. 1999. Study on the role of adhesives in weld-bonded joints. *Welding Journal* 78(8): 275-s to 279-s.

3. Darwish, S. M. H., and Ghanya, A. 2000. Critical assessment of weld-bonded technologies. *Journal of Materials Processing Technology* 105: 221–229.

4. Wang, P. C., Chisholm, S. K., Banas, G., and Lawrence, F. V., Jr. 1995. Role of failure mode, resistance spot weld and adhesive on the fatigue behavior of weld-bonded aluminum. *Welding Journal* 74(2): 41-s to 47-s.

5. Darwish, S. M. H. 2003. Weld-bonding strengthens and balances the stresses in spot-welded dissimilar thickness joints. *Journal of Materials Processing Technology* 134(3): 352–362.

6. Goncalves, V. M., and Martins, P. A. F. 2006. Static and fatigue performance of weld-bonded stainless steel joints. *Materials and Manufacturing Processes* 21: 774–778.

7. Long, X., and Khanna, S. K. 2008. Fatigue performance of spot welded and weld bonded advanced high strength steel sheets. *Science and Technology of Welding and Joining* 13(3): 241–247.

8. Sam, S., and Shome, M. 2010. Static and fatigue performance of weld bonded dual phase steel sheets. *Science and Technology of Welding and Joining* 15(3): 242–247.

9. Vogler, M., and Sheppard, S. 1993. Electrical contact resistance under high loads and elevated temperatures. *Welding Journal* 72: 231-s to 298-s.

10. Thornton, P. H., Krause, A. R., and Davies, R.G. 1996. Contact resistances in spot welding. *Welding Journal* 75(12): 402-s to 412-s.

11. Song, Q. F., Zhang, W. Q., and Bay, N. 2005. An experimental study determines the electrical contact resistance in resistance welding. *Welding Journal* 84(5): 73-s to 76-s.

12. Rogeona, P., Carrea, P., Costaa, J., Sibilia, G., and Saindrenanb, G. 2008. Characterization of electrical contact conditions in spot welding assemblies. *Journal of Materials Processing Technology* 195: 117–124.

13. Cho, Y. J., and Rhee, S. H. 2000. New technology for measuring dynamic resistance and estimation strength in resistance spot welding. *Measurement Science and Technology* 11(8): 1173–1178.

14. Garza, F., and Das, M. 2001. On real time monitoring and control of resistance spot welds using dynamic resistance signatures. *Midwest Symposium on Circuits and Systems* 1: 41–44.

15. Cho, Y., and Rhee, S. 2002. Primary circuit dynamic resistance monitoring and its application to quality estimation during resistance spot welding. *Welding Journal* 81(6): 104-s to 111-s.

16. Ma, C., Bhole, S. D., Chen, D. L., Lee, A., Biro, E., and Boudreau, G. 2006. Expulsion monitoring in spot welded advanced high strength automotive steels. *Science and Technology of Welding and Joining* 11(4): 480–487.

17. ANSI/AWS/SAE/D8.9–97, *Recommended practices for test methods for evaluating the resistance spot welding behavior of automotive sheet steel materials*, 1997. Miami, Fla.: American Welding Society.

18. ASM International. 1998. *Metals Handbook Desk Edition*.

19. Shen, J., Zhang, Y. S., Lai, X. M., and Wang, P. C. 2011. Modeling of resistance spot welding of multiple stacks of steel sheets. *Materials and Design* 32(2): 550–560.

20. Santos, I. O., Zhang, W., Goncalves, V. M., Bay, N., and Martins, P. A. F. 2004. Weld bonding of stainless steel. *International Journal of Machine Tool & Manufacture* 44: 1431–1439.